

Study of Contact Temperature During Polishing of Zinc Plate with Ultrasonic Vibration Using Single Pole Magnetic Abrasive Finishing

Gurpreet Singh¹, Kheelraj Pandey^{2*}, Ashwani Sharma³, Chitra Bajpai⁴, Gaurav Raj Pandey⁵

Abstract

The present work scrutinizes the impact of ultrasonic vibration on the contact temperature during polishing zinc plates with Single Pole Magnetic Abrasive Finishing (SPMAF). The efficacy and eminence of FMAB finishing are pointedly influenced by heat generation at the interaction point, as raised up temperatures can lead to the deprivation of abrasive elements or the bonding material inside the brush, which leads to the fading its overall effectiveness. The magnetic abrasive particles (MAPs) play a vital role in the machining region to achieve high-precision surface finishing. Ultrasonic vibrations boost the performance of the flexible magnetic abrasive brush (FMAB), which affects the material exclusion and thermal behaviour. Key aspects analysed include polishing-speed (250–1250 RPM), feed-rate (1.5–5.5 mm/sec), working-gap (4–6 mm), and temperature variations at the workpiece-brush interaction during finishing. The study objectives are to establish a connection between process parameters, contact temperature, and finishing efficiency. Experimental consequences indicate that ultrasonic vibrations influence heat generation within the brush, which affects machining performance and surface features. The results contribute to improving SPMAF parameters for improved thermal management, surface quality in precision engineering applications.

Keywords: Single pole magnetic abrasive finishing (SPMAF), flexible magnetic abrasive brush (FMAB), contact temperature (CT), surface texture analysis, and ultrasonic-vibration-assisted magnetic abrasive finishing.

INTRODUCTION

The high precision finishing technique called single pole magnetic abrasive finishing can be used in automotive, aerospace, medical and electronic industries. For example, the fine finishing of engine and gear box in automobile industries, to enhance the surface integrity of turbine blades in aerospace industries, biocompatible and polished surgical tools and implants in medical industries, ultrafine finishing of micro components, semiconductors and microdevices for electronic industries. Single pole magnetic abrasive finishing may find an effective technique for attaining high quality surface texture in various industrial and aerospace applications. A connection between process parameters, contact temperature, and finishing effectiveness by examining the variables such as brush speed, gap of working in the finishing zone has been experimentally studied to see the effect of heat generated at the contact interface. The investigation helps to reveal in optimizing the finishing process for maximum efficiency with minimum thermal damage to polished zinc surface.

*Author for Correspondence
Kheelraj Pandey

1UG Scholar, Department of Mechanical Engineering, Amity University, Lucknow, Uttar Pradesh, India
2,3Assistant Professor, Department of Mechanical Engineering, Amity University, Lucknow, Uttar Pradesh, India
4Assistant Professor, Department of Mechanical Engineering, Shri Ramswaroop Memorial College of Engineering and Management, Lucknow, Uttar Pradesh, India
5PG Scholar, Department of Mechanical Engineering, Amity University, Lucknow, Uttar Pradesh, India

Received Date: September 23, 2025
Accepted Date: October 30, 2025
Published Date: April 23, 2026

Citation: Gurpreet Singh, Kheelraj Pandey, Ashwani Sharma, Chitra Bajpai, Gaurav Raj Pandey. Study of Contact Temperature During Polishing of Zinc Plate with Ultrasonic Vibration Using Single Pole Magnetic Abrasive Finishing. Journal of Polymer & Composites. 2026; 14(Special Issue 2): S1239–S1247p.

Advancements in intelligent control, sustainable materials, and hybrid systems are expected to shape the future of MAF and expand its applicability across domains. Based on the past research; Shinmura et al. [1] conducted pioneering research on the fundamental mechanisms of SR improvement in magnetic abrasive finishing. Their work established that the finishing pressure generated by magnetic forces controls the interaction between abrasive particles and the workpiece surface, resulting in micro-cutting actions that selectively remove peaks from surface irregularities. They demonstrated that MAF could reduce SR from several micrometers to manometer levels under optimized conditions. Yamaguchi and Shinmura [2] examined the influence of magnetic field distribution on surface finish quality, demonstrating that uniform magnetic flux density across the working area contributes to consistent SR. Their research provided design guidelines for magnetic field generators to achieve homogeneous surface finishes across complex geometries. Jain et al. [3] investigated the micro-mechanics of surface modification in MAF processes. Using scanning electron microscopy and surface profilometry, they documented how abrasive particles create microscopic cutting paths that progressively reduce surface asperities. Their work established correlations between the finishing time and SR improvement, identifying characteristic three-phase behaviour: rapid initial improvement, steady-state reduction, and eventual saturation. Chang et al. [4] examined the influence of abrasive grain size on final SR. Their systematic experiments with different mesh sizes established that finer abrasives produced better surface finishes but at reduced material removal rates. They proposed a two-stage finishing strategy using progressively finer abrasives to optimize processing efficiency. Mori et al. [5] investigated nanoscale finishing capabilities of advanced MAF processes. Using specially formulated ultra-fine abrasive media and precisely controlled magnetic fields, they demonstrated capabilities for reducing SR to Ra values below 10 nm on metallic mirror components. Singh et al. [6] investigated abrasive concentration effects on SR outcomes in MAF. Their research established optimal volumetric concentrations (typically 25-35% by volume) that balanced sufficient cutting action with proper magnetic brush formation. Higher concentrations resulted in diminished improvement due to restricted particle mobility, while lower concentrations provided insufficient cutting action. Yin and Shinmura [7] investigated surface finishing characteristics of titanium alloys using modified magnetic abrasive processes. Their research demonstrated that conventional MAF techniques required adaptation for these materials, with specially formulated abrasive compositions achieving SR reductions from initial Ra values of 0.5–0.8 μm to final values of 0.04–0.07 μm . Judal and Yadava [8] combined electrochemical principles with magnetic abrasive finishing to create a hybrid process for difficult-to-machine materials. Their approach leveraged electrochemical reactions to soften the surface layer while simultaneous MAF action removed the reaction products, resulting in SR improvements up to 95% from initial values. Xing et al. [9] made a study on Pulse Electrolytic Magnetic Abrasive Finishing (P-EMAF) of SUS304 stainless steel using rectangular wave pulse voltage explored the effects of varying frequencies (1 Hz–1 kHz) and duty ratios (25%–75%) on SR and material removal. Optimal results were achieved at 1 Hz and 50% duty ratio with 6 V, showing improved surface finish and higher efficiency compared to traditional MAF. This pioneering research highlights the potential of P-EMAF in advanced surface finishing. Yamaguchi et al. [10] conducted extensive studies on SR improvement in hardened steel components using MAF. Their research demonstrated capabilities for reducing SR from initial Ra values of 0.8–1.2 μm to final values of 0.02–0.05 μm . They identified optimal processing conditions for different steel grades based on hardness levels and initial surface conditions. Mishra et al. [11] established and authenticated a model to determine work-brush interface temperature in magnetic abrasive finishing, examining effects of speed, magnetic flux, and material properties on heat generation and surface excellence. Singh et al. [12] scrutinized temperature distribution in magnetic abrasive finishing of aluminium 6060 using finite element modeling. The study discovered that temperature rises with spindle speed, magnetic flux density, and working gap decrease. Higher temperatures exaggerated surface finish quality. Findings emphasized optimizing parameters to stabilize efficient finishing with nominal thermal damage. Sharma et al. [13] showed preliminary experiments on work-brush interface temperature through single-pole magnetic abrasive finishing of silicon wafers. Outcomes exhibited temperature rise with increased rotational speed and magnetic flux. Conclusions highlight the implication of thermal monitoring in SPMAF to avoid wafer damage and confirm precise finishing quality. The process integrated with ultrasonic assistance has been used to monitor the thermal behaviour on the finished work sample.

In the present study, a novel experimental approach has been developed and optimized for evaluating the contact temperature during the polishing of zinc plates using ultrasonic vibration-assisted single pole magnetic abrasive finishing (SPMAF). To the best of our knowledge, no prior work has been reported in the literature that combines ultrasonic vibration, magnetic abrasive finishing, and single pole tool configuration specifically for temperature analysis at the work-tool interface.

METHODOLOGY

Slurry Preparation and Experimental Framework

The experimental setup shown in Figure 1 was used for polishing a zinc plate. It consists of a hollow cylinder containing a permanent disc magnet (NdFeB) with a diameter of 25 mm, which serves as the polishing tool. An iron block, consisting of a stack of iron plates, is mounted on the movable platform of the machine to provide horizontal feed to the workpiece. A vibrating platform with a polishing tray is located on top of the iron block. The tool is mounted on a CNC milling machine, while the workpiece is held between a single-pole permanent magnet and the iron block. For polishing, a brush is created between the workpiece and the magnetic pole due to the magnetic field generated by single-pole magnet and iron block. The flexible magnetic abrasive brush (FMAB) is fabricated by mixing magnetic abrasive particles (MAPs) consisting of 30% aluminium oxide and 70% iron particles. As the magnet rotates, the FMAB also rotates, effectively removing the peaks on the workpiece surface. A chemical solution is poured onto the surface of the workpiece to facilitate etching and easy material removal. This solution is prepared from 2.5 ml of nitric acid (HNO_3), 2 ml of hydrogen peroxide (H_2O_2), 5 g of aluminium oxide powder (Al_2O_3), and 50 ml of distilled water. Nitric acid is used to weaken the atomic bonds on the zinc surface without altering its crystal lattice, while hydrogen peroxide forms a protective passive layer that prevents oxidation. This solution also acts as a cooling and lubricating medium, controlling friction and heat generation between the FMAB and the zinc workpiece during the finishing process. The solution is applied at five-minute intervals to maintain continuous polishing performance. During the 30-minute polishing process, the workpiece temperature is manually measured using an infrared thermometer by directing the laser onto the zinc surface every three minutes. Monitoring the contact temperature at the interface is important because it reveals the interaction between the FMAB and the zinc workpiece and helps determine the optimal amount of polishing agent during polishing. Continuous temperature monitoring reduces the risk of surface erosion during the process. As friction increases between the FMAB and the zinc surface, the contact temperature also rises, requiring a higher amount of polishing agent in the working interval to reduce surface defects caused by the abrasive cutting action.

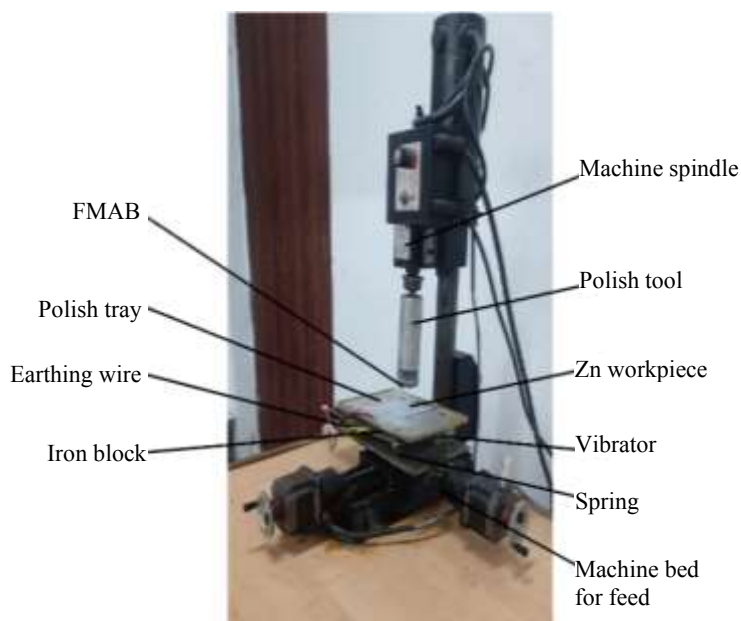


Figure 1. SPMAF experimental setup.

Table 1. Process parameter particulars.

Experimental process parameters symbols	Description of experimental process parameters	Level on the lower side	Level on the higher side
X1	'Tool speed' in RPM	250	1250
X2	'Working Gap' in millimeters	4	6
X3	'Feed rate' in mm/s	1.5	5.5
X4	'Pulse on time' in min.	1	5

Table 2. Measured the value of contact temp. of and % improvement in surface roughness (with initial roughness of raw sample being 0.29 μm) of zinc workpiece for individually investigational test.

Exp. no.	Tool speed (RPM)	Working gap (mm)	Feed rate (mm/s)	Pulse on time(min)	Contact temp. ($^{\circ}\text{C}$)	% Improvement in surface roughness
1	250	4	5.5	5	24.7	41.03
2	250	4	1.5	5	24.8	44.83
3	250	6	5.5	5	22.9	41.72
4	250	4	1.5	1	24.6	42.41
5	1250	4	1.5	1	25.4	50.69
6	1250	4	5.5	5	25.1	51.38
7	1250	6	5.5	5	24.3	49.66
8	1250	6	1.5	1	24.5	48.28
9	250	4	5.5	1	24.4	40
10	1250	6	1.5	5	24.9	49.31
11	250	6	1.5	5	24.3	42.07
12	250	6	1.5	1	23.2	39.66
13	1250	6	5.5	1	24.0	48.62
14	1250	4	5.5	1	25.0	51.03
15	250	6	5.5	1	22.8	41.38
16	1250	4	1.5	5	25.7	51.72

Planning of Experiment

The experiment investigated key process parameters—tool speed, working gap, workpiece feed rate, and pulse-on time—using an L-16 factorial design to assess the contact temperature of a zinc workpiece. Table 1 presents the chosen parameters and their corresponding levels. Contact temperature measurements were carried out with an infrared thermometer between the FMAB and zinc plate, the data was recorded after every 2 minutes for a total period of 20 minutes. The contact temperature values at the edge of flexible magnetic abrasive brush (FMAB) and workpiece i.e., Zinc obtained for each trial, is summarized in Table 2. Further the percentage improvement in the surface roughness for each experimental trail corresponding to the value of contact temperature because he localized heating at the interface of FMAB and zinc workpiece is also highlighted in Table 2.

Examination of Experimental Data

The experiments were conducted by means of an L-16 factorial plan in Minitab 17. A model linear in nature was joint into the design, is subsequently adapted in the following response Equation.1. The regression equation obtained from the model analysis is shown by Equation 2

$$CT (^{\circ}\text{C}) = \alpha_o + \sum_{i=1}^n \beta_i x_i + \epsilon \quad (1)$$

In this study, CT signifies the temperature between workpiece and the device (FMAB tool) of the zinc workpiece, while n denotes the number of experimental parameters. The coefficient β_i defines their influence, x_i denotes the linear terms of process-variable quantity, and ϵ accounts for error term occurring randomly. The statistics of the Experiments were evaluated through Analysis-of-Variance (ANOVA), with Table 3 presenting the ANOVA results for CT. To further explore process parameter effects on CT, a multivariable regression equation (Equation 1) was formulated.

Table 3. ANOVA of regression equation.

Source	DF	Adj. SS	Adj. MS	'F'-Value	'p'-Value	Observation
Model	4	9.6725	2.41813	31.48	0.00	
Linear	4	9.6725	2.41813	31.48	0.00	$F_{(0.05,11,4)}^{standard} = 5.93$ $F^{model} = 31.48$ $F^{model} > F_{(0.05,11,15)}^{standard}$ $\Rightarrow 31.58 > 5.93$ The statistical model for the contact temperature is accurate
X_1	1	3.2400	3.24000	42.18	0.00	
X_2	1	4.8400	4.84000	63.81	0.00	
X_3	1	1.1025	1.10250	14.35	0.003	
X_4	1	0.4900	0.49000	6.38	0.028	
Error	11	0.8450	0.07682			
Total	15	10.5175				

A correlation between CT and process parameters (X_1, X_2, X_3, X_4), with an adjusted R^2 of 89.04 % at a 95% confidence level and a minimal error of 0.59 shown accuracy in statistical evaluation of experimental data.

$$CT (^{\circ}C) = 26.684 + 0.0009000X_1 - 0.5500 X_2 - 0.1312X_3 - 0.0875X_4 \quad (2)$$

RESULT AND DISCUSSION

Effect of Tool Speed on Contact Temperature

Figure 2(a) illustrates the association between polishing speed and surface roughness. The figure indicates that as polishing speed rises, the contact temperature also rises. This increase can be attributed to the higher surface friction generated at elevated speeds, leading to a rise in contact temperature (CT).

Effect of Working Gap on Contact Temperature

The influence of the working-gap on contact temperature is depicted in Figure 2(b). The figure demonstrates that as the working gap increases, the CT of polished silicon decreases. This effect is due to the reduction in magnetic flux concentration in a larger working space, which lowers the penetration strength of magnetic abrasive particles (MAPs) in the polishing area. Consequently, a smaller amount of friction arises between the abrasive particles and the surface, leading to a lower temperature.

Effect of Workpiece Feed Rate on Contact Temperature

Figure 2(c) illustrates the influence of workpiece feed-rate on CT. The figure reveals that increasing the feed-rate results in the elevation workpiece temperature. This temperature rise occurs due to the enlarged friction amid the abrasive particles and the workpiece at higher feed rates, leading to an elevated CT.

Effect-of- Pulse on time on Contact Temperature

The contact temperature between FMAB and zinc material is seen to increase with the rise in pulse on time as revealed in Figure 2(d). The reason can be that the increase in pulse on time causes excitation in the abrasive particles resulting in greater penetration causing material removal from the workpiece surface and. allows faster heat removal from the cutting zone preventing micro cracks and formation of heat affected zone on the workpiece surface.

Optimum Result by Means of Fmincon Function

The optimization method involved using equation 1 which was found afterward regression analysis and can be articulated as:

Maximize Contact Temperature (CT)

s.t;

$$250(\text{rpm}) \leq X_1 \leq 1250(\text{rpm})$$

$$4(\text{mm}) \leq X_2 \leq 6(\text{mm})$$

$$1.5(\text{mm/s}) \leq X_3 \leq 5.5(\text{mm/s})$$

$$1(\text{min}) \leq X_4 \leq 5(\text{min})$$

The Figure 3 illustrate the maximum Contact Temperature at optimum limits highlighted in Table 4, as obtained from equation (2) and resembles the Optimum values of Contact Temperature. The optimum values of process parameters have been obtained with the help of Fmincon tool-kit available in MATLAB 2013. The regression equation (2) was employed, with predefined constrictions resulting from the experimental investigation on condition that in Table 2. Using the same constrictions and conditions, the extreme value of a contact temperature is 25.85 ± 0.59 .

The optimum limits were:

$$X_1 = 12500 \text{ rpm}$$

$$X_2 = 4 \text{ mm}$$

$$X_3 = 1.5 \text{ mm/sec}$$

$$X_4 = 5 \text{ min}$$

Prediction of temperature distribution and nature of strain on finished surface of zinc material

Figure 4(a) shows the SEM micrograph of unfinished zinc workpiece which was subjected to finishing at optimum parameters resembled in Table 4. The SEM micrograph of finished sample at magnification of 2500X shown in Figure 4(b). The Pixel intensities of the finished sample corresponding to Figure 4(b) are shown with the help of Histogram in Figure 4(c). Figure 4(d) shows the nature of diffraction lines corresponding to the crystal lattice variation due to the changes in the crystal lattice corresponding to the changes in the interplanar spacing between the crystal lattices. In the current situation the condition shown in Figure 4(d)-2 prevails. There appear uniform changes in lines with as shown in Figure 4(d)-2 and hence micro strains and uniform temperature distribution exist on the finished surface while executing the SPMAF process.

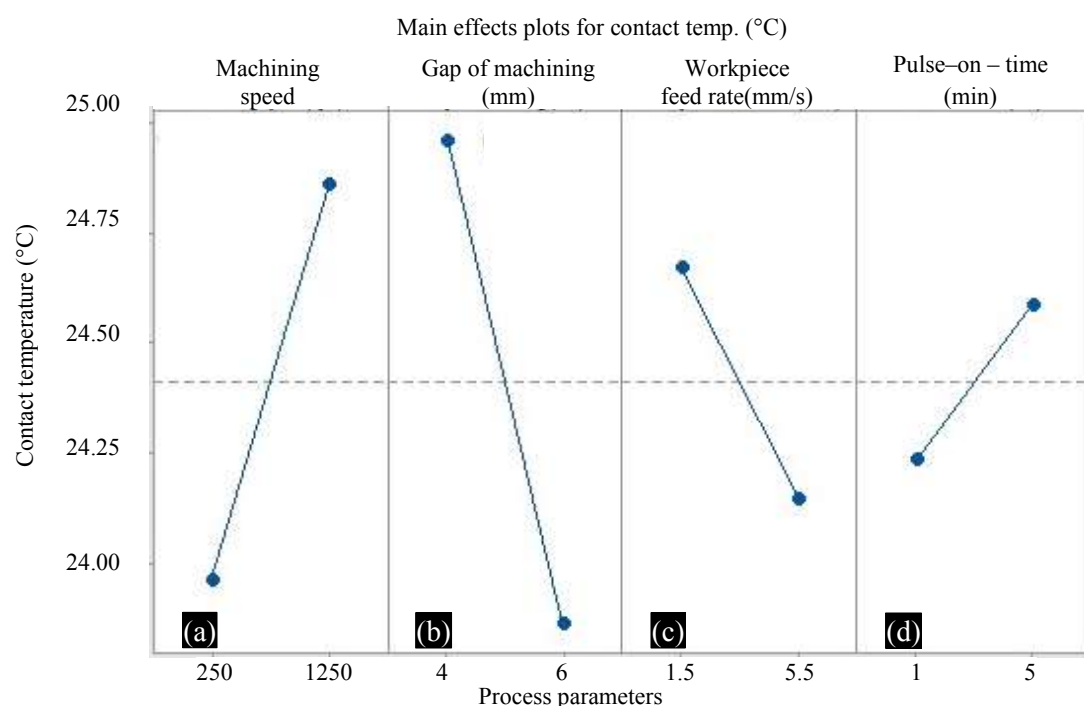


Figure 2. Variation of contact temperature with process parameters.

Table 4. Optimization parameters for maximum contact temperature.

Tool Speed (X_1) rpm	Working-Gap (X_2) mm	Feed-rate (X_3) mm/sec	Pulse on time (min)	CT ($^{\circ}$ C) from model	Experimental CT ($^{\circ}$ C)
1250	4	1.5	5	25.85 \pm 0.59	25.7

Considering the Bragg's equation, the micro strains are tensile in nature as the shift is towards the left side which implies that the value of ' θ ' decreases which decreases the value of ' $\sin \theta$ ' and hence the distance between atomic layers (d) increases.

$$d = \frac{n\lambda}{2 \sin \theta} \quad (3)$$

Here (n) is an integer, (λ) is the wavelength of X-ray beam, (d) is the interplanar distance amid the atomic layers and (θ) is the angle of incidence of the X-ray.

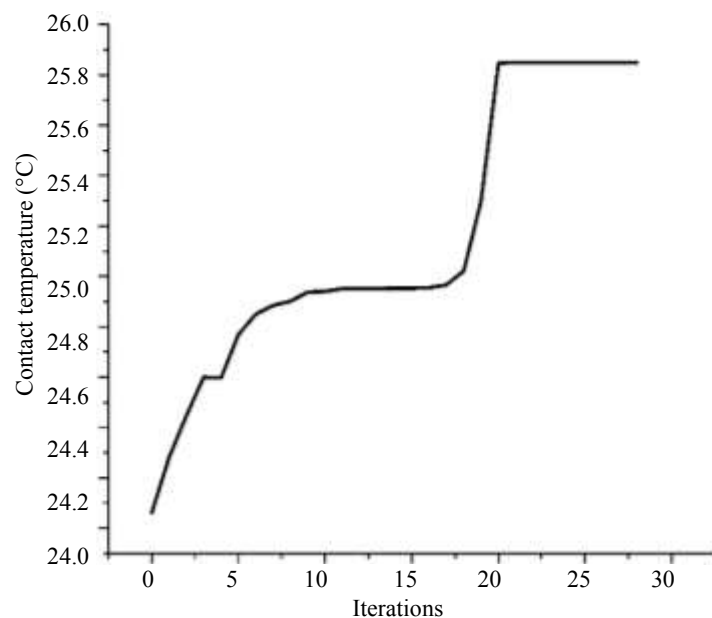


Figure 3. Optimum standards of contact temperature.

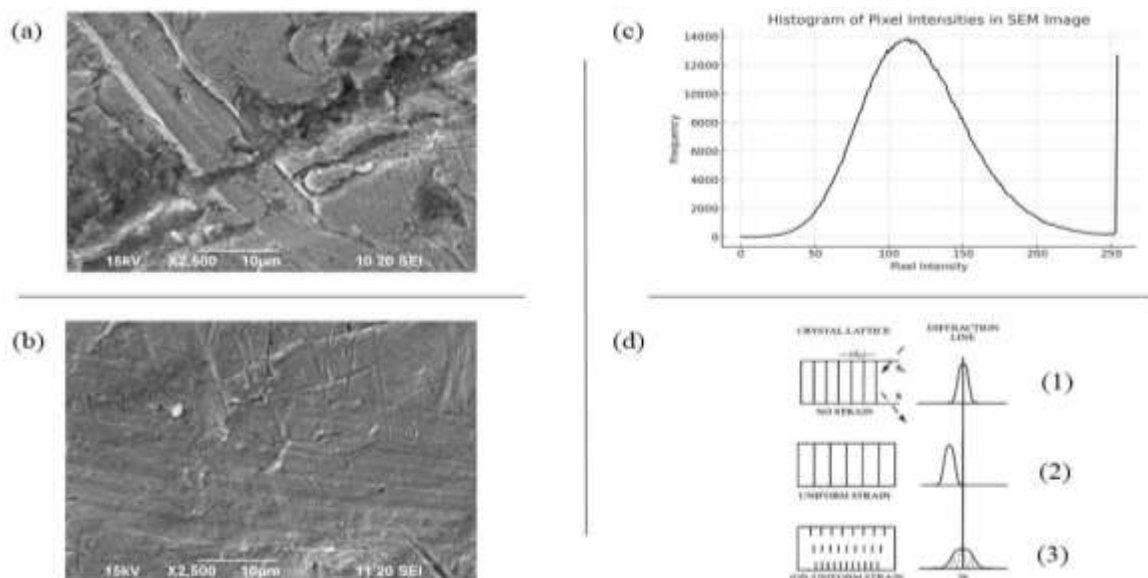


Figure 4. SEM micrograph showing temperature distribution and nature of strain on finished surface of zinc material.

CONCLUSIONS

The application of ultrasonic vibrations in SP-MAF significantly increases overall effectiveness by influencing the contact temperature, improving material removal, and refining surface quality. Higher tool speed and feed increase the contact temperature due to increased surface friction and heat generation. Conversely, a larger working gap leads to a decrease in contact temperature because it reduces the magnetic flux density and thus limits heat accumulation. Extending the pulse duration increases the activity of the abrasive particles, resulting in higher material removal and a higher contact temperature, and enabling more efficient heat dissipation from the polishing area. Scanning electron microscopy (SEM) investigations showed a significant improvement in surface stability and a reduction in surface defects after the finishing process. Overall, monitoring the thermal behaviour is necessary to optimize the SP-MAF parameters and avoid thermal problems such as the formation of microcracks or heat-affected zones.

Declaration of Interest

The authors confirm that there are no financial or personal relationships that could have influenced the research presented in this paper.

Ethics Approval

N/a

REFERENCE

1. Shinmura T, Takazawa K, Hatano E. Study on magnetic abrasive finishing. *CIRP Annals Manufacturing Technology*. 1990;39(1):325-8. [https://doi.org/10.1016/S0007-8506\(07\)61064-6](https://doi.org/10.1016/S0007-8506(07)61064-6)
2. Yamaguchi H, Shinmura T. Study of the surface modification resulting from an internal magnetic abrasive finishing process. *Wear*. 2000;225-229:246-55. [https://doi.org/10.1016/S0043-1648\(99\)00013-7](https://doi.org/10.1016/S0043-1648(99)00013-7)
3. Jain VK, Kumar P, Behera PK, Jayswal SC. Effect of working gap and circumferential speed on the performance of magnetic abrasive finishing process. *Wear*. 2001;250(1-12):384-90. [https://doi.org/10.1016/S0043-1648\(01\)00642-1](https://doi.org/10.1016/S0043-1648(01)00642-1)
4. Chang GW, Yan BH, Hsu RT. Study on cylindrical magnetic abrasive finishing using unbonded magnetic abrasives. *International Journal of Machine Tools and Manufacture*. 2002;42(5):575-83. [https://doi.org/10.1016/S0890-6955\(01\)00153-5](https://doi.org/10.1016/S0890-6955(01)00153-5)
5. Mori T, Hirota K, Kawashima Y. Clarification of magnetic abrasive finishing mechanism. *Journal of Material Processing Technology*. 2003;143-144:682-6. [https://doi.org/10.1016/S0924-0136\(03\)00410-2](https://doi.org/10.1016/S0924-0136(03)00410-2)
6. Singh DK, Jain VK, Raghuram V. Parametric study of magnetic abrasive finishing process. *Journal of Material Processing Technology*. 2004;149(1-3):22-9. <https://doi.org/10.1016/j.jmatprotec.2003.10.030>
7. Yin S, Shinmura T. A comparative study: Polishing characteristics and its mechanisms of three vibration modes in vibration-assisted magnetic abrasive polishing. *International Journal of Machine Tools and Manufacture* 2004;44(4):383-90. <https://doi.org/10.1016/j.ijmachtools.2003.10.002>
8. Judal KB, Yadava V. Electrochemical magnetic abrasive machining of AISI304 stainless steel tubes. *International Journal Precision Engineering and Manufacture*. 2013; 14:37-43. <https://doi.org/10.1007/s12541-013-0006-1>
9. Xing B, Zou Y, Tojo M. Study on Magnetic Abrasive Finishing Combined with Electrolytic Process—Precision Surface Finishing for SUS 304 Stainless Steel Using Pulse Voltage. *Journal of Manufacturing and Material Processing*. 2022;6(1):14. <https://doi.org/10.3390/jmmp6010014>
10. Yamaguchi H, Srivastava AK, Tan MA, Riveros RE, Hashimoto F. Magnetic abrasive finishing of cutting tools for machining of titanium alloys. *CIRP Annals Manufacturing Technology*. 2012;61(1):311-4. <https://doi.org/10.1016/j.cirp.2012.03.066>
11. Mishra V, Goel H, Mulik RS, Pandey PM. Determining work-brush interface temperature in magnetic abrasive finishing process. *Journal of Manufacturing Processes*. 2014 Apr 1;16(2):248-56. <https://doi.org/10.1016/j.jmapro.2013.10.004>

12. Singh RK, Gangwar S, Singh DK. On the temperature analysis of magnetic abrasive finishing of aluminium 6060 using finite element method. *Machining Science and Technology*. 2020 Nov 22;25(2):177-208. <https://doi.org/10.1080/10910344.2020.1815036>
13. Sharma A, Pandey K, Sood AK. Preliminary Experimental Investigation into Work Brush Temperature on Silicon Wafer Using Single Pole Magnetic Abrasive Finishing (SPMAF). In *International Conference on Scientific and Technological Advances in Materials for Energy Storage and Conversions 2023* Jul 20 (pp. 569-579). Singapore: Springer Nature Singapore. https://doi.org/10.1007/978-981-97-3173-2_39